Journal of Structural Geology, Vol. 1, No. 4, 1979, pp. 275–282.

0191-8141/79/1201-0275 $02.00/0

Structural analysis of sheath-folds in a meta-chert from the Western Italian Alps

L. D. MINNIGH

Departemento de geologia, U.F.R.N., Campus Universitário, 59.000 Natal-RN, Brazil

(Received 12 October 1979; accepted in revised form 2 January 1980)

Abstract—A detailed meso- and microscopic structural investigation of a laminated manganiferous meta-chert from the Western Italian Alps has resulted in the recognition of five deformation phases. During the third phase large subhorizontal shear movements took place, resulting in reorientation of pre-existing structures and sheath-fold formation. This was accompanied by a decrease in pressure, reflected by the zoning of blue-amphiboles and by microboudinage and the formation of stretching cracks in minerals. The orientation of amphiboles, together with some evidence from quartz *c*-axis fabrics suggest that the deformation took place by simple shear. During the late stages of sheath-fold formation the deformation became non-rotational.

INTRODUCTION

THE STRUCTURES described in this paper occur in a layer of meta-chert which is associated with impure marbles, carbonate-bearing schists, and leucocratic and albite-chlorite gneisses in the Orco valley (NW Italy) (Fig. 1). The geology of the area has been described by Minnigh (1978). Similar rocks found in nearby areas (Elter 1971, Bearth 1976) are interpreted by Debenedetti (1965) as belonging to the ophiolitic schistes lustrés of Malm age.

The finely laminated meta-chert allows complex fold interference patterns to be recognized. Based on these interference patterns and other overprinting relationships five phases of deformation have been identified. Successive events are referred to as D_1, D_2, etc., axial surfaces are referred to as S_1, S_2, etc. and fold hinge lines as l_1, l_2, etc.

GEOMETRY OF STRUCTURAL ELEMENTS AND THEIR RELATIVE AGES

Evidence for the earliest deformation phase (D_1) comes from rare intrafolial folds. The associated foliation is called S_1 and is commonly isoclinally folded by D_2 folds (Figs. 2a & b). A pronounced lineation, defined by elongate quartz aggregates, is developed parallel to the D_2-fold hinges. This lineation is referred to as l_2.

In several outcrops D_1- and D_2-folds are refolded by D_3-folds to form tight similar or mushroom-shaped interference patterns (Fig. 2c). The third deformation phase folded the l_2-lineation (Fig. 2d). The hinges of D_3-folds are generally curvilinear. Occasionally the curvature is such that attenuated domes have been developed. Cross sections perpendicular to the central axis of these domes give rise to oval patterns (Fig. 3). Structures of this type have recently been described as sheath-folds (Carreras *et al.* 1977, Quinquis *et al.* 1978). Textural evidence (see later) demonstrates that blue-amphiboles grew during the formation of the sheath-folds. These amphiboles define a lineation (l_3) which is usually parallel to l_2. Occasionally however, l_3 is observed to be bent within the foliation plane, in the same way as the curvilinear D_3-fold hinges.

D_4 produced asymmetric folds resulting in commonly observed fold interference patterns (Fig. 2e). D_5-folds are kinks, boxfolds or open folds. Axes of both D_4 and D_5 folds are subparallel to l_2. Structural elements from the mapped area are illustrated in Fig. 4.

MESOSCOPIC ASPECTS OF SHEATH-FOLDS

The central axis of a sheath fold is referred to as X, and the long and short axes of the elliptical section perpendicular to X are referred to as Y and Z respectively. The sides of the sheath-fold which are more or less parallel to the XY-plane and subparallel to the main foliation are called the limbs of a sheath-fold.

Two hand-specimens were used for an investigation of meso- and microstructures. Specimen I is a sheath-fold with X = 13 cm, Y = 13.5 cm and Z = 4.5 cm. A l_2-lineation on the limbs lies in the XZ-plane. On the XZ-section the fold is similar in style.

Specimen II is illustrated in Fig. 2(d). One limb contains a strongly developed l_2-lineation and the other a folded amphibole lineation. The XZ-section perpen- asymmetric, similar fold profile. An oval pattern with Y = 4 cm and Z = 0.6 cm is present in a section perpendicular to l_2 and about 12 cm away from the curvilinear l_3-hinge. It indicates the presence of a sheathfold in which the X-axis is of unknown length.

The distribution of the amphiboles in the folded lineation gives some insight into the deformation mechanisms that operated. Specimen II was cut into serial sections at 0.5 mm intervals perpendicular to the X-axis of the sheath-fold for a study of the orientation of the amphiboles in three dimensions. The outlines of the amphiboles were drawn and then stored by a computer in which they are available for orientation measurements [for details of the computer program see Westbroek *et al.* (1976) and Hesper, in Schoneveld (1979)]. Amphibole orientations are presented in Fig. 5. A pattern similar to that illustrated is obtained when a population of passive markers with an initially preferred orientation is subjected to simple shear (Minnigh 1979).

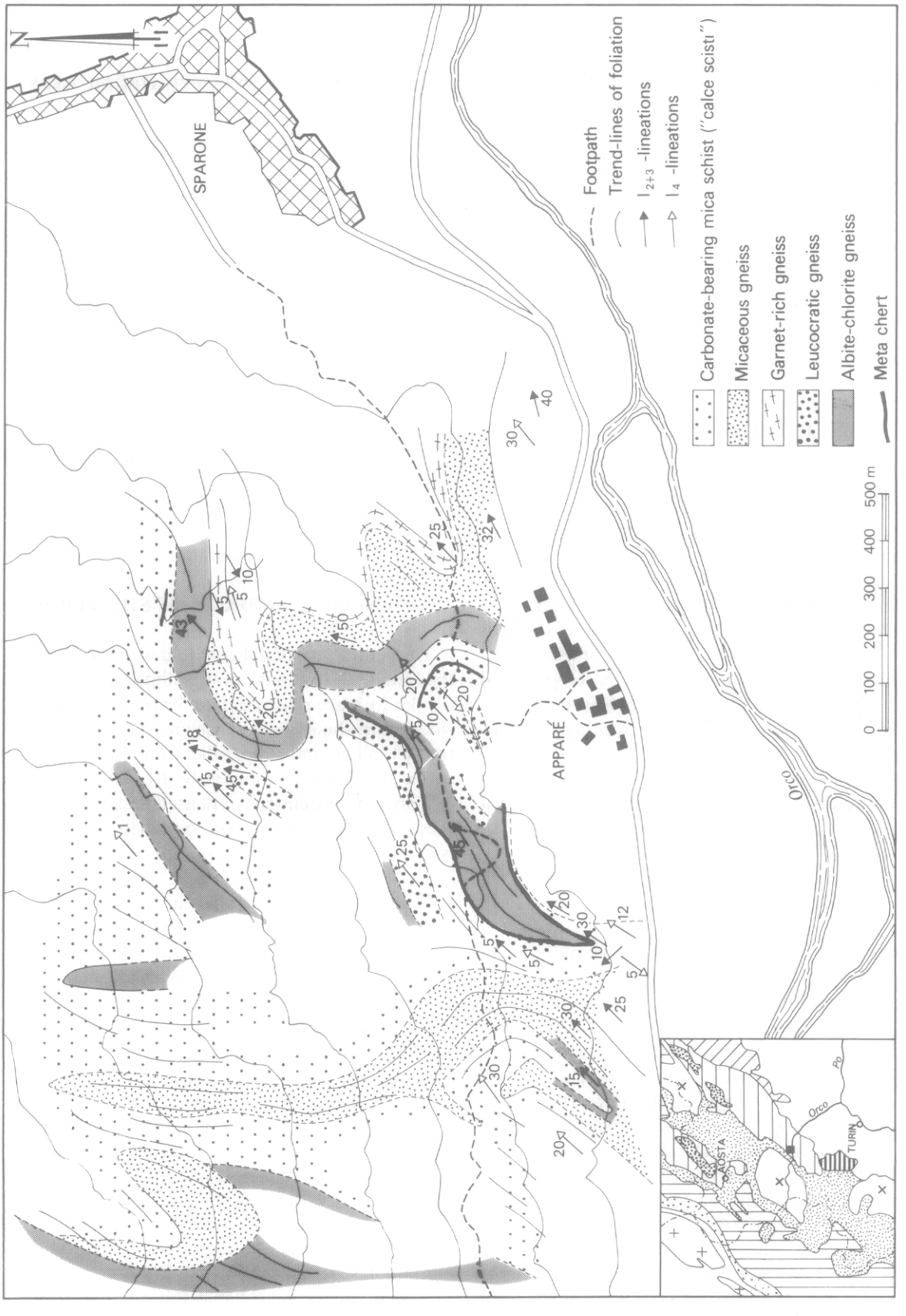

Fig. 1. Map of principal lithological units including the meta-chert layer. Inset shows the location of the study area within the Western Alps.

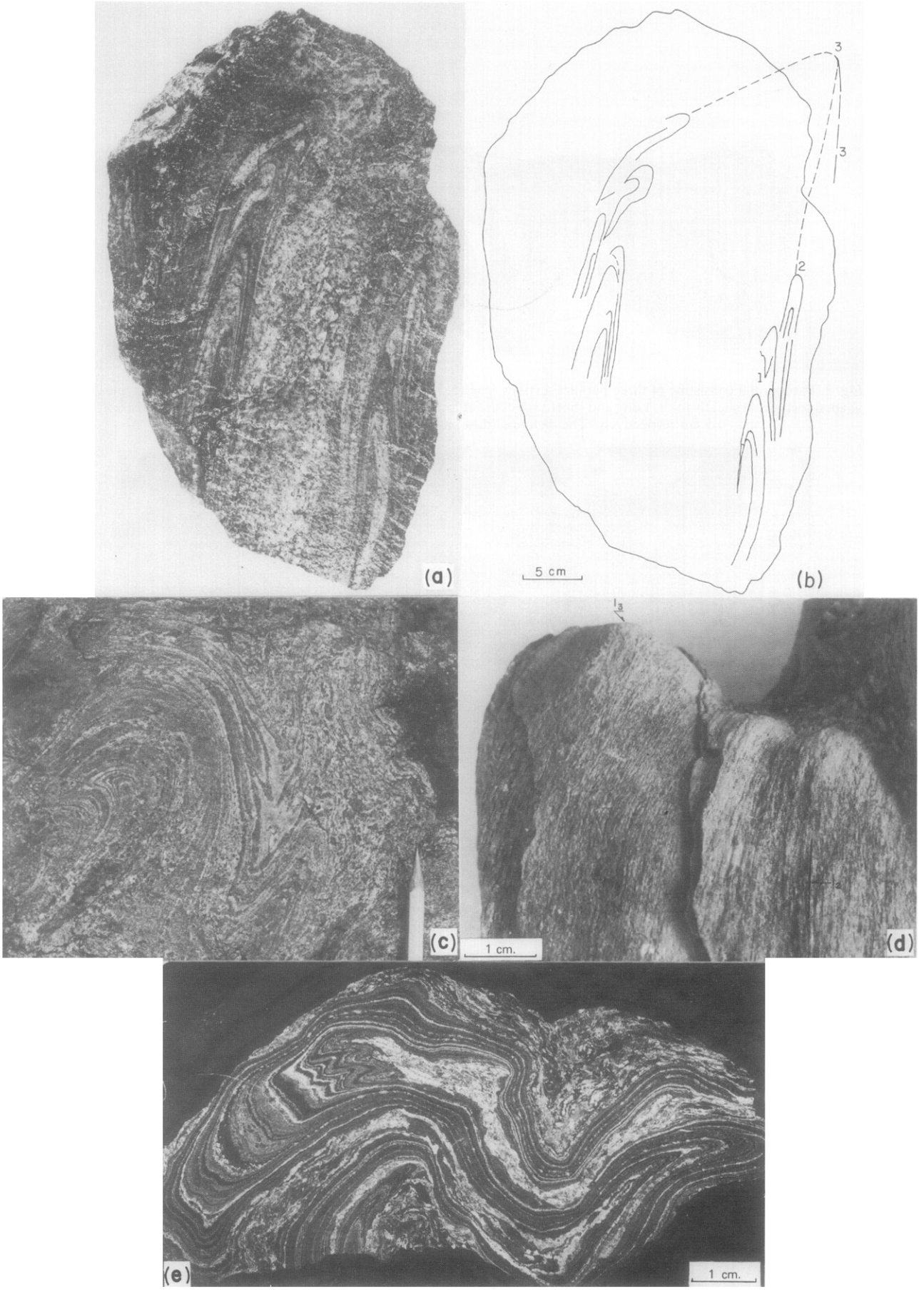

Fig. 2. Various types of fold interference patterns in the meta-chert. (a) Hand-specimen (sampled by P. F. Williams), where isoclinal D_1- and D_2-folds are refolded in a symmetrical pattern by D_3-folds. (b) Sketch of the fold interference pattern of (a). Numbers refer to the hinge lines of the fold generations. The D_3-fold hinge is illustrated schematically. (c) Outcrop of impure chert near Aparé showing a mushroom-shaped fold interference pattern related to D_3. (d) A fine and pronounced l_2-lineation at a high angle to a curved D_3-fold hinge is continuous round the hinge. The axial surface of the fold is subparallel to the plane of the photograph. (e) Negative print of a thin-section showing a typical interference pattern resulting from the refolding of isoclinal D_2-folds during D_4. The repetition of the lamination within the layer is related to D_1, although hinge lines are difficult to recognize.

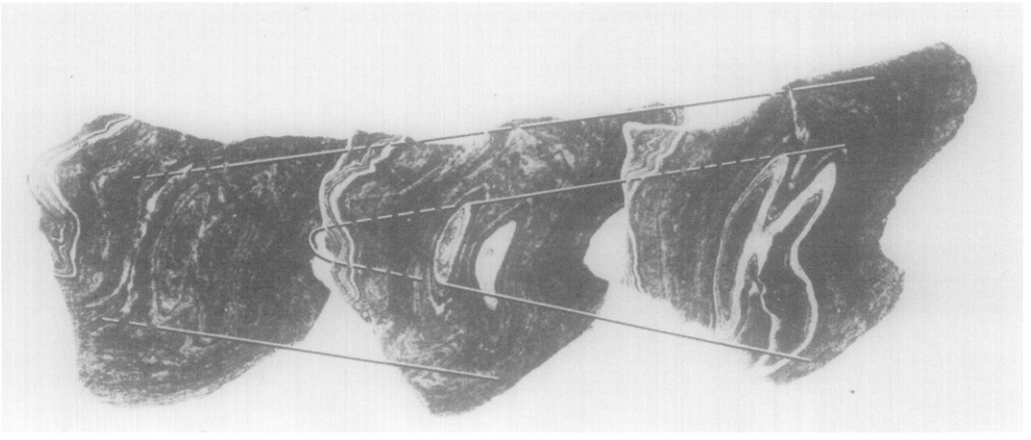

Fig. 3. Photograph consisting of three parallel sections (each 5.5 cm apart) through a hand-specimen showing typical eye-shaped sections of sheath-folds. Long and short axes of the elliptical base (right section) of the inner sheath-fold are 8.5 and 0.5 cm respectively. The distance from base to nose of the fold is about 8 cm.

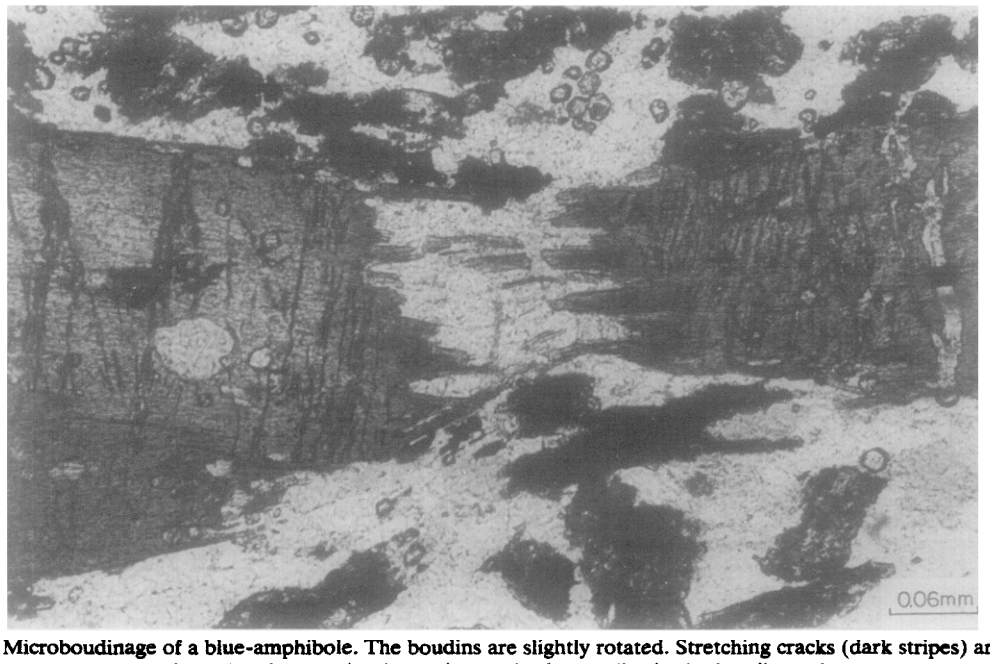

Fig. 8. Microboudinage of a blue-amphibole. The boudins are slightly rotated. Stretching cracks (dark stripes) are abundant. A colour zoning is continuous in the needles in the boudin neck.

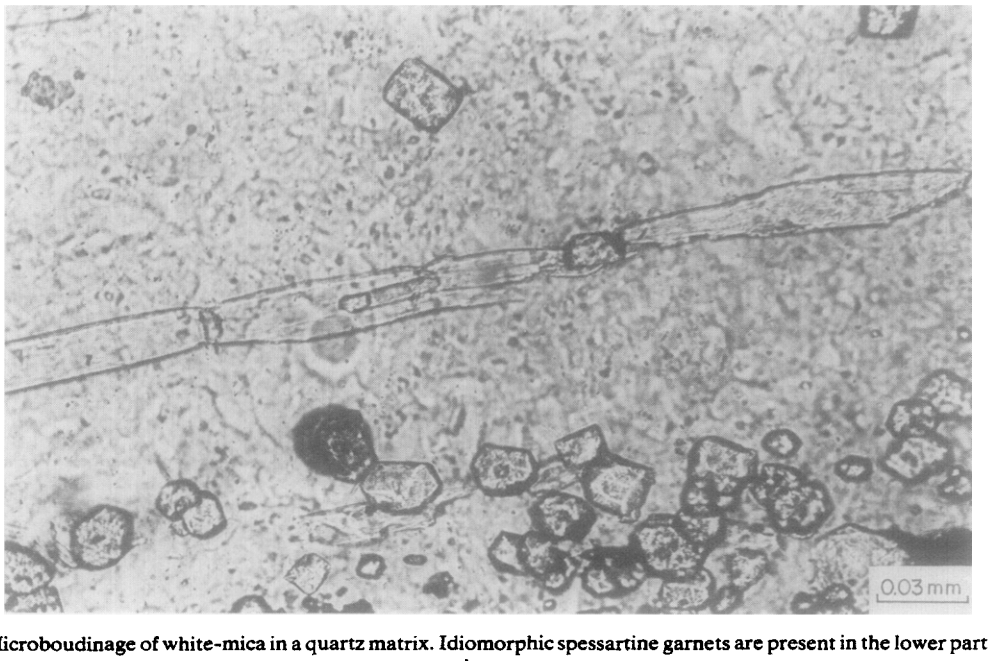

Fig. 9. Microboudinage of white-mica in a quartz matrix. Idiomorphic spessartine garnets are present in the lower part of the photo.

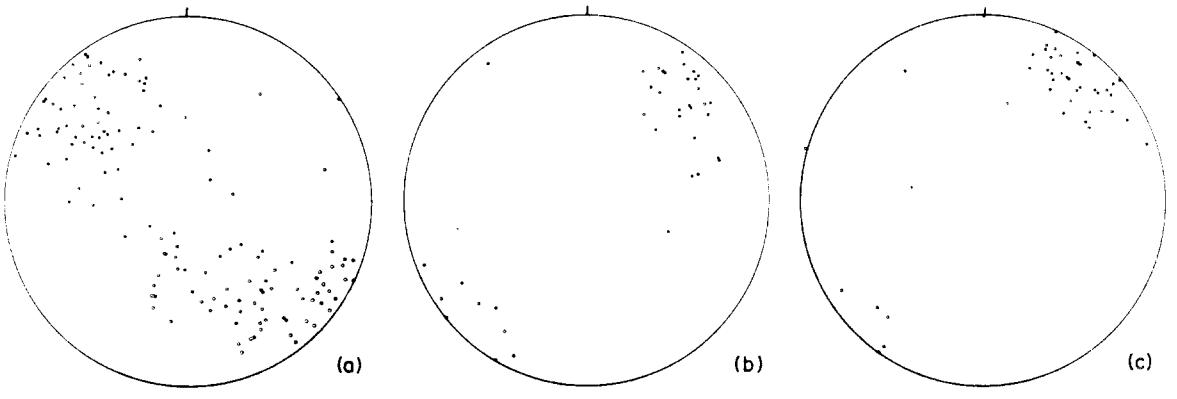

Fig. 4. (a) 142 poles to the main foliation plotted on an equal-area net (lower hemisphere). The poles define a broad great-circle girdle with two poorly-defined maxima. (b) 38 l_2-lineations, defining a maximum plunging approximately 045°/18°. (c) 48 l_4-lineations defining a maximum plunging approximately 058°/16°.

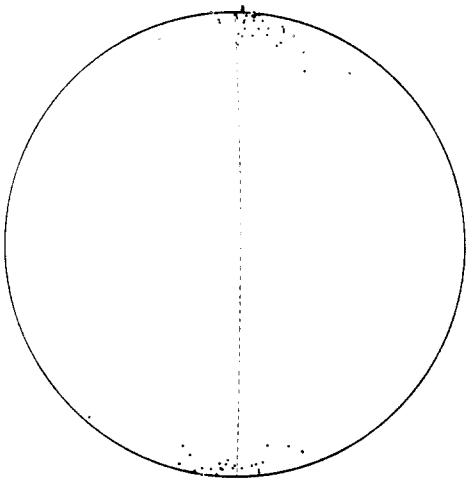

Fig. 5. Stereogram showing long axes of 58 amphiboles of hand-specimen II. The possible orientation of the shear plane is indicated by the pecked great-circle.

MICROSCOPIC ASPECTS OF SHEATH-FOLDS

Quartz fabrics

The meta-chert is composed of quartz, fine-grained idiomorphic spessartine garnet and small amounts of white-mica, blue-amphibole and opaque minerals. The layering is defined by alternations of quartz- and garnet-rich layers. Micas and amphiboles are normally distributed throughout the rock.

In quartz-rich layers large areas are made of a number of quartz grains with similar crystallographic orientations. These grains themselves are composed of poorly defined subgrains, giving the large grains an irregular undulose extinction. The shapes of the large grains are variable and the boundaries are serrated or sutured. Quartz *c*-axes were measured in small (generally 1×2 mm) areas, parallel to the *X*-axis of the sheath-fold of specimen I. Several features can be distinguished from the fabric diagrams (Fig. 6); (a) the fabric is not uniform in the different areas of the limbs and (b) cleft girdle patterns are present in the core of the fold. The small differences between individual plots are probably the result of interactions with an older fabric, or the deformation was heterogeneous on the scale of the thin-section, or they are due to D_4 or D_5.

Quartz *c*-axes were also studied in a thin-section cut parallel to the *X*-axis of the sheath-fold of specimen II (Fig. 7). Here, the diagrams show similar *c*-axis patterns throughout the specimen and they are different from specimen I.

Recent work, using computer programs to simulate the development of quartz fabrics (Lister 1974, Hobbs *et al.* 1976, Lister *et al.* 1978, Lister & Price 1978), gives some insight into deformation mechanisms in quartz-rich rocks. Although complex natural processes are difficult to simulate, the natural fabric diagrams are compared with those proposed on theoretical grounds by Lister. The cleft girdle patterns in the core of the fold of specimen I show similarities with diagrams based on a coaxial extension perpendicular to the girdles (see Lister *et al.* 1978, fig. 14c), that is parallel to the *X*-axis of the sheath-fold. The diagrams of Fig. 7 are nearly identical with models based on progressive simple shear (see Lister & Price 1978, fig. 18).

Microboudinage and zoning of blue-amphiboles

In this account a distinction is made between boundinage and stretching cracks. Where there is necking the structure is called boudinage, where separation is planar, it is called a stretching crack.

Boudinage of blue-amphibole (Fig. 8), white-mica (Fig. 9) and epidote has been observed. Small blue-green amphibole needles are present in the necks of amphibole boudins. The *c*-axes of amphiboles generally lie in the foliation. The orientations of *a* and *b*-axes are variable. Usually the amphiboles are gradationally zoned with a light blue core and a dark blue-green rim. Microprobe analyses (Minnigh 1979) indicate that the colour zoning corresponds exactly with a chemical zoning; the light blue core being relatively enriched in Mg^{2+} and impovorished in Fe^{2+}. Boudins on both limbs of sheath-folds are rotated in the same sense.

Stretching cracks

Stretching cracks are common in blue-amphibole,

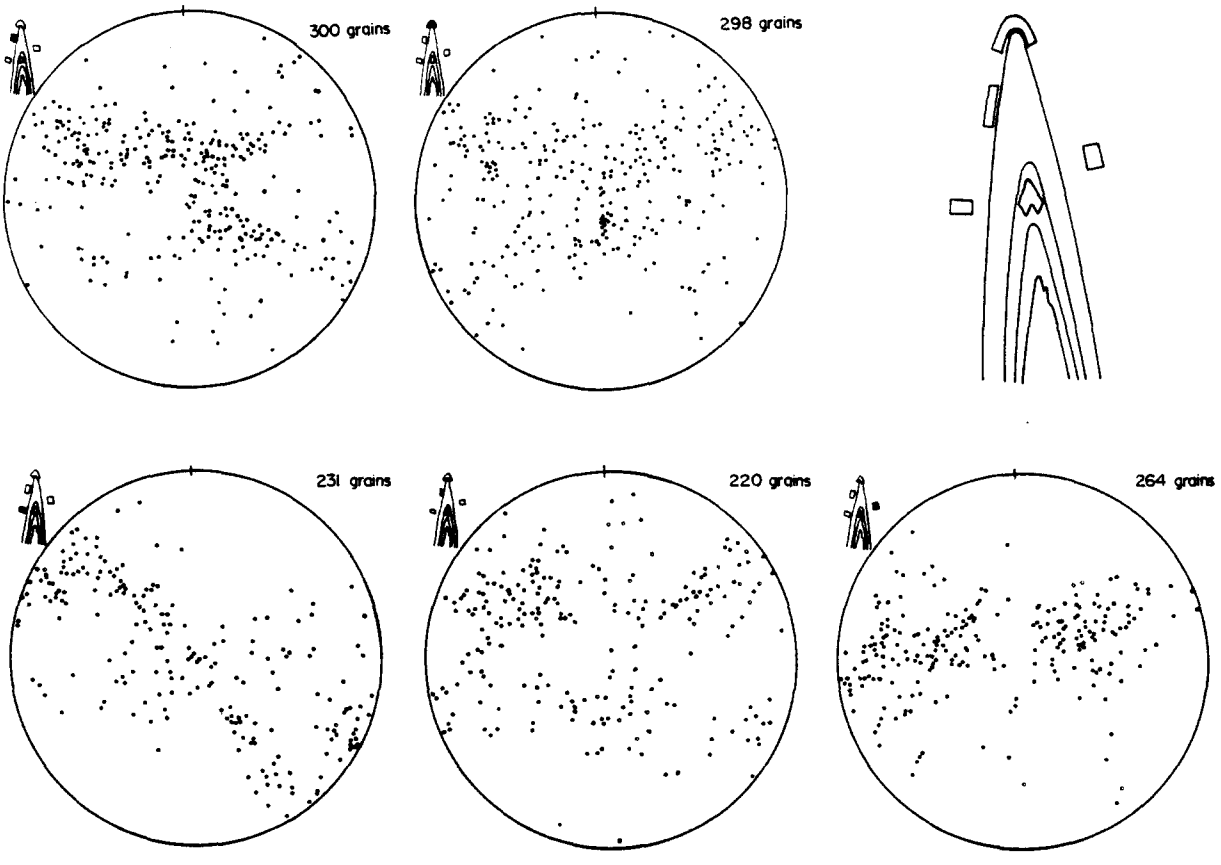

Fig. 6. Quartz *c*-axis fabrics from specimen I. The general pattern is a cleft girdle, with minor variations and concentrations.

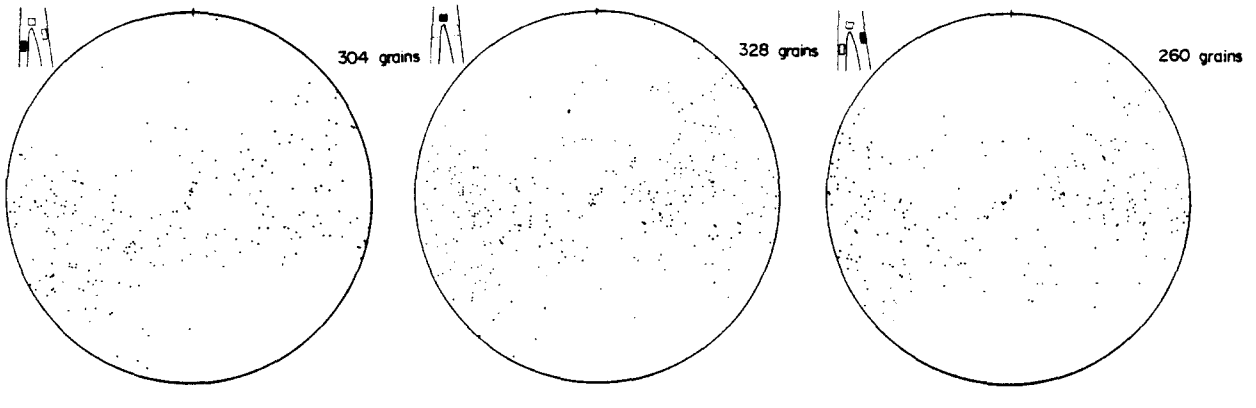

Fig. 7. Quartz *c*-axis fabrics from specimen II showing asymmetrical girdles. In the different areas the fabrics are the same.

garnet, epidote, apatite and white-mica. There is no apparent relationship between crystallographic directions and the orientations of cracks. In amphiboles for example, cracks through basal as well as elongate sections occur in roughly the same orientation. The cracks vary in width from 0 – 0.015 mm and are filled with a fine-grained mineral aggregate of chlorite, white-mica, green amphibole and magnetite.

The orientations of cracks in amphibole crystals from specimen II were measured using the U-stage, on a thin-section parallel to the *X*-axis of the sheath-fold. White-micas show the same deformation features as the amphiboles, and they are parallel to the amphiboles. In order to define the foliation the (001)-mica cleavage was measured, and the results are given in Fig. 10 (a).

Orientations of cracks in amphiboles are compared with those in the equi-dimensional garnets. The cracks have been formed at roughly the same time, because several examples are found where the same crack is continuous through both minerals. Both minerals show the same maximum of preferred orientations of the cracks, although the preferred orientation in garnets is less pronounced (Fig. 10 b). This suggests that no rotation took place during crack formation and that the principal extension direction was perpendicular to the cracks. The maxima are at 9° from the *XY*-plane, which itself is nearly parallel to the foliation.

DISCUSSION

Sheath-folds have recently been described from the Woodroffe thrust in Central Australia (Bell 1978), from

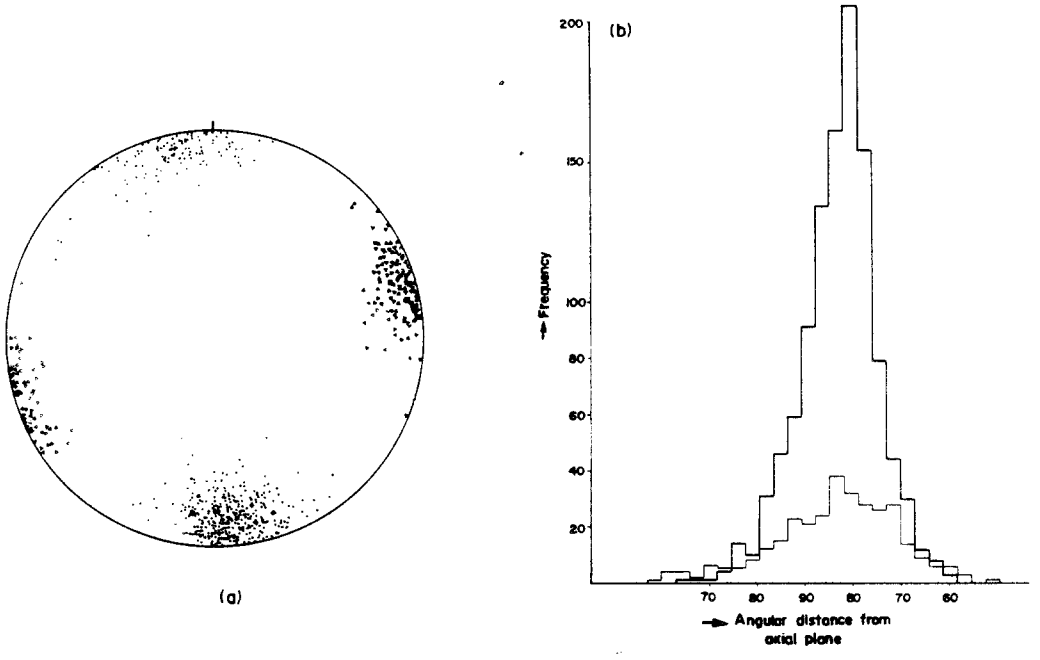

Fig. 10. (a) Stereogram showing poles to stretching cracks in amphiboles (dots) and poles to (001)-cleavage in white-micas (triangles) of specimen II. Note that the crack orientation is not perpendicular to the foliation. (b) Histogram of stretching crack orientations in amphiboles (heavy line) and in garnets (thin line) with respect to the *XY*-plane. Maxima for both minerals coincide and are 9° from the normal to the axial plane.

the Darling Fault in West Australia (Lister & Price 1978), in mylonites from Cabo Creus, Spain (Carreras *et al.* 1977), at the base of the Seve Köli nappe in the Swedish Caledonides (Williams & Zwart 1977), at Ile de Groix (Quinquis *et al.* 1978) and in the South Armorican Shear Zone (Berthé & Brun, in press) both in Brittany. The eye-shaped fold interference patterns described by Dalziel & Bailey (1968) in mylonites from the Grenville front are probably also due to sheath-folds. All these occurrences are characterized by large shear strains. Such strains tend to rotate planar and linear structures into the extension direction (Escher & Watterson 1974, Sanderson 1973). A slightly curved fold hinge subjected to such elongations would be folded, and the resulting structure is a sheath-fold. The original fold could be formed in an earlier deformation phase (Hobbs *et al.* 1976, Williams & Zwart 1978), or could be formed during the extensional deformation itself. The latter mechanism is described by Rhodes & Gayer (1978), Carreras *et al.* (1977), Quinquis *et al.* (1978) and Cobbold & Quinquis (in press), and is illustrated in Fig. 11. Pre-existing anisotropies on the surface or within the layer, together with instabilities in adjacent layers could act as nuclei of folds with slightly curved hinges. At the initial stage of the development of sheath-folds the long axis of the incremental strain ellipsoid is at 45° to the shear plane and therefore the plane which contains the curved hinge is also inclined at 45° to the shear plane. During progressive deformation the plane containing the hinge will be rotated until it is nearly parallel to the shear plane. Cobbold & Quinquis (in press) have simulated this mechanism in experiments with large shear strains (γ above 10) and according to their observations "the formation of sheath folds is hard

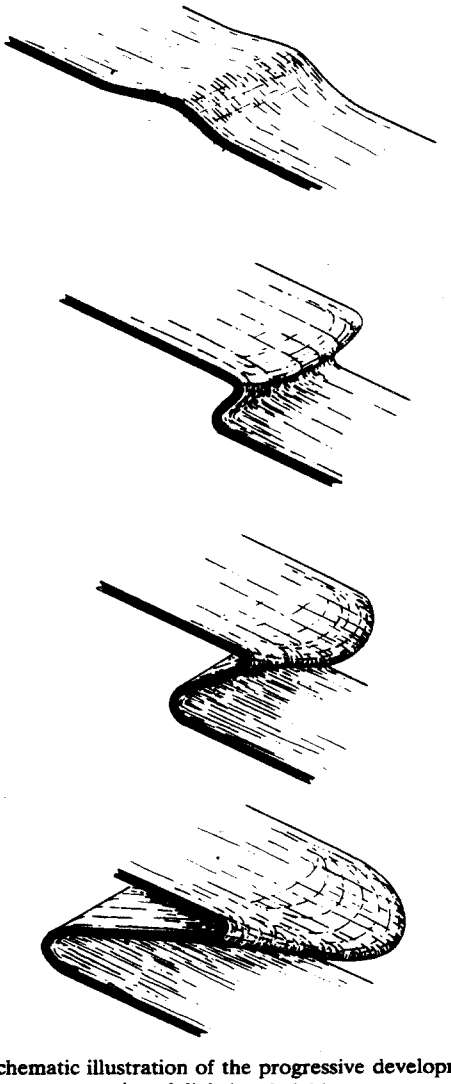

Fig. 11. Schematic illustration of the progressive development of an intrafolial sheath-fold.

to avoid". Probably some other intrafolial folds are also developed in this way.

The large extensions which are necessary for the formation of sheath-folds are caused by coaxial extension, simple shear, or a combination of both mechanisms. A correlation of theoretical and natural patterns of quartz *c*-axes suggests that different deformation mechanisms have operated; coaxial extension in the core of a sheath-fold (Fig. 6), and simple shear (Fig. 7).

All the observed stretching features probably developed during the extensional deformation which formed the sheath-folds. The constant sense of rotation of amphiboles on both limbs of the sheath-fold suggests a progressive simple shear deformation. Also the three-dimensional amphibole distribution (Fig. 5) is in agreement with this. From the same preferred orientation of stretching cracks in amphiboles and in garnets however, it may be concluded that the cracks were formed during a period of coaxial strain, or during an increment of simple shear at a late state of sheath-fold formation.

The colour and chemical zoning of the amphiboles is gradational. Generally, light coloured and Mg-rich Na-amphiboles reflect high pressure-low temperature metamorphism, whereas the more coloured and Mg-poor members indicate a decrease of pressure and/or increase of temperature (see e.g. Miyashiro & Banno 1958, Ernst 1968). The zoning indicates a gradational decrease of metamorphic grade during the several stages of stretching. The different metamorphic minerals filling the boudin-necks and stretching cracks demonstrate that boudinage occurred before cracking. A rise in temperature during the late stages of stretching deformation seems unlikely because the expected increase in ductility appears incompatable with the formation of cracks. A decrease in pressure under fairly constant temperatures is therefore considered more likely.

In conclusion, the formation of sheath-folds in the meta-chert probably began in a high pressure regime subjected to simple shear, possibly parallel to the layering as illustrated in Fig. 11. Pressures gradually decreased and the deformation ended as non-rotational.

The direction of the l_2-lineation indicates the approximate direction of shear. From Fig. 4 it is clear that this was in a subhorizontal NNE–SSW direction. This direction is not disturbed, because the axes of post D_3-folds are subparallel to it. South of Sparone a similar direction of shear has been found in the Lanzo-peridotites (Nicolas *et al.* 1972). This direction is believed to be the movement direction of the African and European plates (Nicolas 1974, 1976).

Acknowledgements—The author is indebted to P. F. Williams, H. J. Zwart, Chr. Schoneveld, G. Gosso, R. J. Lisle, G. S. Lister and J. Wakefield for helpful suggestions and discussions and for reading of various parts of the draft manuscript. Photography and draughting by the staff of the Geological Institute, Leiden is acknowledged.

REFERENCES

Bearth, P. 1976. Zur Gliederung der Bünderschieffer in der Region von Zermatt. *Eclog. geol. Helv.* **69**, 149–161.

Bell, T. H. 1978. Progressive deformation and reorientation of fold axes in a ductile mylonite zone: the Woodroffe thrust. *Tectonophysics* **44**, 285–320.

Berthé, D. & Brun, J. P. in press. Evolution of folds during progressive shear in the South Armorican Shear Zone, France. *J. Struct. Geol.*

Carreras, J., Estrada, A. & White, S. 1977. The effects of folding on the c-axis fabrics of a quartz mylonite. *Tectonophysics* **39**, 3–24.

Cobbold, P. R. & Quinquis, H. in press. Development of sheath folds in shear regimes. *J. Struct. Geol.*

Dalziel, I. W. D. & Bailey, S. W. 1968. Deformed garnets in a mylonite rock from the Grenville front and their tectonic significance. *Am. J. Sci.* **266**, 542–562.

Debenedetti, A. 1965. Il complesso radiolariti—giacimenti di manganese—giacimenti piritoso-cupriferi—rocce a fuchsite, come rappresentante del' Malm nella formazione dei calce scisti—osservazioni nelle Alpi Piemontesi e della Val d' Aosta. *Boll. Soc. geol. ital.* **84**, 131–163.

Elter, G. 1971. Schistes lustrés et ophiolites dela zone piémontaise entre Orco et Doire Baltée (Alpes Graies). Hypothéses sur l'origine des ophiolites. *Geol. Alpine* **47**, 147–169.

Ernst, W. G. 1968 *Amphiboles.* Springer, New York.

Escher, A. & Watterson, J. 1974. Stretching fabrics, folds and crustal shortening. *Tectonophysics* **22**, 223–231.

Hesper, B. 1979. Computer aspects. In: Schoneveld, C. The geometry and significance of inclusion patterns in syntecttonic porphyroblasts. Unpublished Ph.D. thesis, University of Leiden.

Hobbs, B. E., Means, W. D. & Williams, P. F. 1976. *An Outline of Structural Geology.* Wiley, New York.

Lister, G. S. 1974. Theory of deformation fabrics. Unpublished Ph.D. thesis, Australian National University.

Lister, G. S., Patterson, M. S. & Hobbs, B. E. 1978. The simulation of fabric development in plastic deformation and its application to quartzite: the model. *Tectonophysics* **45**, 107–158.

Lister, G. S. & Price, G. P. 1978. Fabric development in a quartz–feldspar mylonite. *Tectonophysics* **49**, 37–78.

Minnigh, L. D. 1978. Petrological outline of an area near Sparone (Orco-Valley, Western Italian Alps). *Leid. geol. Meded.* **51**, 313–329.

Minnigh, L. D. 1979. Petrological and structural investigations of the Sparone area in the Orco valley (Southern Sesia–Lanzo border zone, Western Italian Alps). Unpublished Ph.D. thesis, University of Leiden.

Miyashiro, A. & Banno, S. 1958. Nature of glaucophanitic metamorphism. *Am. J. Sci.* **256**, 97–110.

Nicolas, A. 1974. Mise en place des peridotites de Lanzo (Alpes piémontaises). Relation avec tectonique et metamorphisme alpins. Conséquences géodinamiques. *Schweiz. miner. petrog. Mitt.* **54**, 449–460.

Nicolas, A. 1976. Flow in upper mantle rocks: some geophysical and geodynamic consequences. *Tectonophysics* **32**, 93–106.

Nicolas, A., Bouchez, J. L. & Boudier, F. 1972. Interpretation cinematique des deformations plastiques dans le massif de lherzolite de Lanzo (Alpes Piémontaises)—comparaison avec d'autres massifs. *Tectonophysics* **14**, 143–171.

Quinquis, H., Audren, C., Brun, J. P. & Cobbold, P. R. 1978. Intense progressive shear in Ile de Groix blueschists and compatibility with subduction or obduction. *Nature, Lond.* **273**, 43–45.

Rhodes, S. & Gayer, R. A. 1977. Non-cylindrical folds, linear structures in the *X* direction and mylonite development during translation of the Caledonian Kalak Nappe Complex of Finnmark. *Geol. Mag.* **114**, 329–341.

Sanderson, D. J. 1973. The development of fold axes oblique to the regional trend. *Tectonophysics* **16**, 55–70.

Westbroek, P., Hesper, B. & Neijndorff, F. 1976. Three-dimensional stereographic representation of serial sections. *J. Geol.* **84**, 725–730.

Williams, P. F. & Zwart, H. J. 1977. A model for the development of the Seve-Köli Caledonian nappe complex. In: *Energetics of Geological Processes* (edited by Saxena, S. K. & Bhattacharji, S.). Springer, New York, 169–187.